Quantum confinement induced magnetism in $LaNiO_3$-$LaMnO_3$ superlattices

Shuai Dong[1,2,3] and Elbio Dagotto[1,2]

[1]*Department of Physics and Astronomy, University of Tennessee, Knoxville, Tennessee 37996, USA*

[2]*Materials Science and Technology Division, Oak Ridge National Laboratory, Oak Ridge, Tennessee 37831, USA*

[3]*Department of Physics, Southeast University, Nanjing 211189, China*

(Received 8 February 2013; revised manuscript received 22 March 2013; published 13 May 2013)

The emergence of magnetic reconstructions at the interfaces of oxide heterostructures are often explained via subtle modifications in the electronic densities, exchange couplings, or strain. Here, an additional possible route for induced magnetism is studied in the context of the $(LaNiO_3)_n/(LaMnO_3)_n$ superlattices using a hybrid tight-binding model. In the $LaNiO_3$ region, the induced magnetizations decouple from the intensity of charge leakage from Mn to Ni, but originate from the spin-filtered quantum confinement present in these nanostructures. In general, the induced magnetization is the largest for the (111)-stacking and the weakest for the (001)-stacking superlattices; results compatible with the exchange bias effects reported by Gibert *et al.* [Nat. Mater. **11**, 195 (2012)].

DOI: 10.1103/PhysRevB.87.195116 PACS number(s): 75.70.Cn, 73.21.−b

I. INTRODUCTION

The area of research that focuses on oxide heterostructures is attracting considerable attention because of its importance in the development of quantum devices based on correlated electronic systems.[1–4] Novel physical properties are expected to emerge from electronic reconstruction near the interfaces.[5–8] In particular, the interfacial magnetism can have properties different from those of bulk materials and, in recent years, several investigations revealed various magnetic reconstructions. Their origin can be mainly classified via mechanisms involving modifications in the (1) electronic densities, (2) exchange couplings, and/or (3) strain. For example, mainly due to strain and charge transfer, pure manganite $LaMnO_3/SrMnO_3$ (LMO/SMO) superlattices (SLs) display a variety of magnetic orders[9–14] while, due to modifications in the exchange coupling, distinct magnetic states emerge in the (001), (011), and (111) stacking of $LaFeO_3/LaCrO_3$ SLs.[15–17] Furthermore, the interfacial magnetic orders of $La_{1-x}Sr_xMnO_3$ (LSMO) can be tuned by attaching ferroelectric layers (e.g., LSMO/$BiFeO_3$, LSMO/$BaTiO_3$, and LSMO/PZT), which induce modifications in the interfacial electronic density.[18–23]

Recently, an exchange-bias effect was reported experimentally in $(LaNiO_3)_n/(LaMnO_3)_n$ (LNO/LMO) SLs grown along the (111) axis of a pseudocubic structure.[24] In contrast, no exchange bias was observed in the conventional (001) stacking of LNO/LMO SLs,[24] suggesting a qualitative difference between the (001)- and (111)-stacking directions despite having the same compositions and periodicity (as sketched in Fig. 1). This exchange bias in the (111) stacking is nontrivial since it is well known that LNO is a paramagnetic (PM) metal in its bulk form.[25] Therefore, interesting physical questions arise: what is the origin of the induced magnetic moments in the LNO layers of these SLs? Are they in proportion to the charge transferred across the interfaces, considering that electrons in the LMO layers are spin polarized? Why are the (001) and (111) SLs qualitatively different with regards to their magnetic properties? And what are the expected results for other stacking orientations not yet explored, such as the (011) direction?

In this paper, LNO/LMO SLs will be studied theoretically from the perspective of microscopic models. Our main result is that the experimentally observed magnetism in the LNO layers appears to be mainly caused by *quantum confinement* effects. This induced magnetism is weakly coupled with the actual value of the charge that is transferred from Mn to Ni and depends strongly and nonlinearly on the stacking orientations and the SL periodicity. The underlying physical mechanism discussed here can partially explain the nontrivial exchange bias observed in $(LNO)_n/(LMO)_n$ SLs.

II. MODEL AND METHOD

A hybrid two-orbital tight-binding model is here constructed, containing the Hubbard interaction for both the manganite and nickelate components and the double-exchange (DE) term for the manganite sector only. In past decades, extensive investigations have shown that the two-orbital DE model is a successful model to describe manganites,[26,27] while the two-orbital Hubbard model has also been often employed for the nickelates.[28,29] Recent theoretical studies also used these two models for manganite heterostructures and for LNO bilayers.[12,30–33] For these reasons, our model provides a reasonable starting point to address the LNO/LMO SLs. More explicitly, the model Hamiltonian used here can be written as

$$H = \sum_{\langle ij\rangle,\sigma}^{\alpha\beta} t_{\alpha\beta}^{\vec{r}}(c_{i\alpha\sigma}^{\dagger}c_{j\beta\sigma} + \text{H.c.}) - \frac{J_{\text{H}}}{2}\sum_{i\in\text{Mn}} n_i\vec{\sigma}_i\cdot\vec{S}_i + \sum_{i\in\text{Ni}} V_{\text{Ni}}n_i + H_{\text{Hubbard}}(U,J), \quad (1)$$

where the first term is the standard nearest-neighbor hopping (i.e., the kinetic energy) between orbital α of site i and orbital β of site j. Here the e_g orbitals $d_{x^2-y^2}$ (=1) and $d_{3z^2-r^2}$ (=2) are employed since, in both $LaMnO_3$ and $LaNiO_3$, the transition metals are in the e_g^1 configuration. The (standard) hopping amplitudes are orbital and direction dependent: $t_{11}^x = t_{11}^y = 3t_{22}^x = 3t_{22}^y = -3t_0/4$, $t_{12}^x = t_{21}^x = -t_{12}^y = -t_{21}^y = \sqrt{3}t_0/4$, $t_{11}^z = t_{12}^z = t_{21}^z = 0$, $t_{22}^z = -t_0$. In the present work, the hopping unit t_0 is assumed to be the same for the bonds Mn-O-Mn, Ni-O-Ni, as well as Mn-O-Ni. This approximation is reasonable since density-functional-theory (DFT) studies of $LaNiO_3$ led to[33] $t_0 \sim 0.6$ eV while a very close result

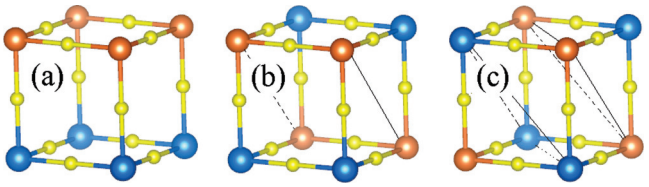

FIG. 1. (Color online) The three stacking configurations of perovskite SLs (period $n = 1$) studied here: (a) (001), (b) (011), (c) (111). Blue and brown balls are the transition metals, such as Ni and Mn, while the yellow balls are the oxygens. The A-site cation (e.g., La) is not shown.

$t_0 \sim 0.5 \sim 0.6$ eV was found for $LaMnO_3$.[34] Moreover, t_0 will be taken as the energy unit in this work.

The Hund's coupling second term affects only the Mn ions that are in a high-spin t_{2g}^3 configuration. Then the spin-up and -down levels are split by J_H in $LaMnO_3$. Here, J_H is set to be $4t_0$ (~2–2.4 eV)[26] which is large enough to induce half-metal behavior in manganites. In contrast, the Ni ions are in the t_{2g}^6 configuration. Then the spin-up and -down levels are degenerate in $LaNiO_3$, suggesting a nonmagnetic background.

The third term is the on-site e_g potential difference between Ni and Mn. Considering the potential of the Mn's spin-up level as the zero of reference, the potential of the Mn's spin-down level becomes J_H due to the Hund coupling, while the potential V_{Ni} for the Ni levels will be varied as a parameter in our investigations.

The last term is the standard Hubbard interaction for multi-orbital models acting in the whole lattice, with the parameters U (intraorbital Coulomb repulsion) and J (interorbital Hund exchange).[28,29,31–33] This term is here treated using the Hartree mean-field approximation, which is a quite reasonable starting point to handle Hubbard interactions in these systems, according to previous literature.[31–33] The widely used ratio $J = U/4$ is used, and U is tuned as a parameter for both the manganite and nickelate layers. In reality, the value of U may be different between Mn and Ni. However, the physical consequences of U are not important for the e_g sector of manganites: at least in the Hartree mean-field approximation it has been shown that a large J_H coupling already plays a similar role.[35] Then, to avoid a large number of tunable parameters, here the same U is applied to both the manganite and nickelate layers. $LaNiO_3$ is a PM metal, implying a weak U (otherwise it would become magnetically ordered).[24] Then, in the present work U will be tuned between 0 and $2t_0$. Note that larger values of U, such as $3t_0$, have also been tested and the results do not alter our physical conclusions qualitatively.

Partially due to strain, the ground state of LMO ultrathin films with nearly cubic structure grown on $SrTiO_3$ is ferromagnetic (FM).[9,12,24] In addition, e_g electrons leak from Mn to Ni, altering the Mn valence to $+(3 + \delta)$, further driving the LMO layers to a FM state according to the phase diagram of manganites.[26] Thus, the t_{2g} spin background of the Mn layers is set here as FM unless explicitly noted. For this first study, lattice distortions are neglected; an assumption also used in other previous theoretical studies of $LaNiO_3$-based heterostructures.[31–33] Then, Eq. (1) is solved self-consistently at zero temperature on $4 \times 4 \times L$ lattices with twisted boundary conditions,[14,23] where L is determined by the period of each SL.

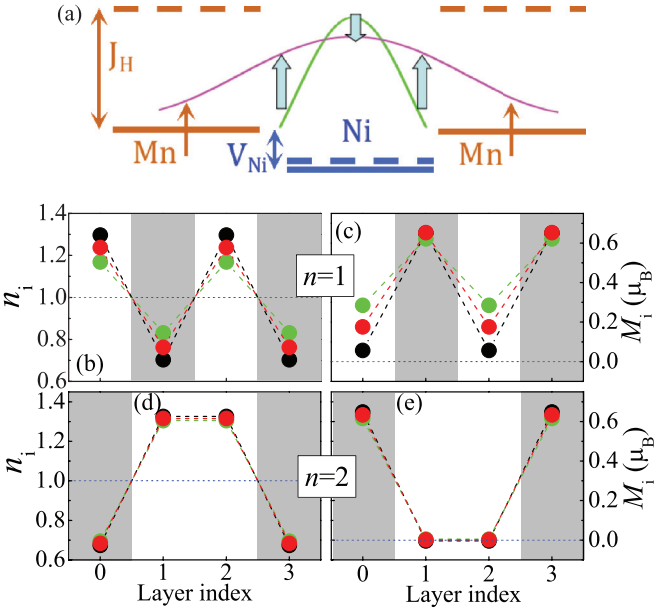

FIG. 2. (Color online) (a) Sketch of spin-filtered quantum confinement. Solid and broken lines denote the spin-up and spin-down levels, which are degenerate for Ni but split by J_H for Mn. $V_{Ni} < 0$ implies lower Ni levels. Pink and green curves are the sketch of spin-up and spin-down e_g electron densities. (b)–(e) The e_g-density profiles (left) and e_g magnetization (right) of SLs at $V_{Ni} = U = 0$. Black is for (001)-, red is for (011)-, green is for (111)-stacking SLs. Gray is for LMO and white is for LNO.

III. RESULTS AND DISCUSSION

A. Noncorrelated limit

First, the simplest case ($U = 0$, $V_{Ni} = 0$) is studied. This noncorrelated limit ($U = 0$) is useful to clarify the underlying physics, and $V_{Ni} = 0$ means that there is no confinement for the spin-up channel although the spin-down channel is still confined due to the large Hund J_H barrier, as sketched in Fig. 2(a). To start the discussion, let us focus first on short periodic ($n \leqslant 2$) SLs because it will be shown below that the induced magnetism is uniform in this case.

Previous DFT calculations[24] indicated that at the interface the e_g electrons transfer from Mn^{3+} to Ni^{3+}. As shown in Figs. 2(b) and 2(d), our calculations are in agreement since, even at $V_{Ni} = 0$, e_g electrons leak from Mn^{3+} to Ni^{3+}. This is because the e_g levels in Mn's sites are spin polarized, pushing the Fermi level of LMO to higher energies since only spin-up bands can be occupied while spin-down bands are almost empty. By contrast, in LNO both the spin-up and -down bands can be filled, accommodating more electrons with a lower Fermi level.

The charge transfer from LMO to LNO depends on both the period n as well as the stacking orientations. For the $n = 1$ case (Fig. 1), the (001)/(011)/(111)-stacking SLs have two/four/six Ni-Mn but four/two/zero Mn-Mn or Ni-Ni nearest neighbors per site. For other cases ($n \geqslant 2$), each interfacial Mn (Ni) ion has one/two/three Ni (Mn) nearest

neighbors but five/four/three Mn (Ni) nearest neighbors in the (001)/(011)/(111)-stacking SLs. Therefore, naively, the charge transfer from Mn to Ni may be the strongest (weakest) in the SLs with (111) stacking [(001) stacking] since they have the most (least) Mn-Ni bonds.

However, this naive scenario is too simplistic. For example, for $n = 2$ the charge transferred to LNO is nonzero, and almost identical, for the three orientations. But at the same time the associated LNO magnetization is nearly vanishing. Moreover, in the $n = 1$ case the charge transferred to the Ni layers is the highest for the (001) stacking, yet the magnetization is the *smallest* for the same stacking. Therefore, the intensity of charge leakage is not in linear proportion to the induced magnetization.

According to Fig. 2, there are several interesting features in the induced magnetism of LNO in these short-period SLs. In the $n = 1$ SLs, the (111) stacking shows the most prominent induced magnetization, while the (001) stacking is nearly nonmagnetic and the (011) stacking interpolates between (001) and (111). In the $n = 2$ cases, the induced magnetism of Ni is almost zero irrespective of the stacking orientations

These features also imply that the induced magnetism is indeed *not* simply directly correlated with the leakage of spin-polarized charge. For a better understanding of our results consider instead the band structures of our SLs. As shown in Fig. 3, the spin-resolved density of states (DOS) at the Ni layers shows that the spin-up and -down channels are notoriously different. Due to the high spin polarization of manganites, the spin-up e_g electrons spread much farther in the SLs than the spin-down e_g electrons, which are mostly confined to the LNO layers. From this perspective, the LMO layers act as atomic-scale spin filters, causing the local band structures of the LNO layers to be quite different between the spin-up and -down channels. Furthermore, this quantum confinement severely depends on the stacking orientations and periodicity. The confinement is the most effective (i.e., with

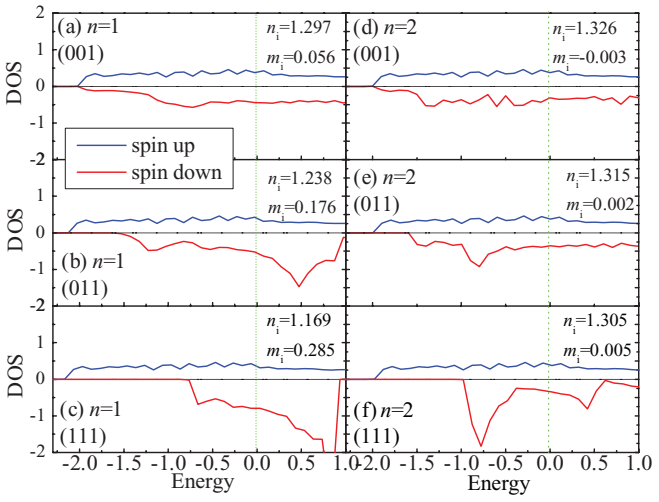

FIG. 3. (Color online) (a)–(f) Spin-resolved density of states of Ni. The Fermi level is at 0. Here $U = 0$ and $V_{Ni} = 0$. Left panels are for $n = 1$, right panels are for $n = 2$. Upper panels are for (001) stacking, middle panels are for (011) stacking, and lower panels are for (111) stacking. The e_g electron densities and magnetism are also shown.

the narrowest spin-down bands) in the (111)-stacking SLs due to their minimum number of Ni-Ni bonds. By contrast, the spin-down bands in the (001) stacking are broader and close to the spin-up channel.

In the $n = 1$ case, the narrowing of the spin-down bands due to quantum confinement gives rise to the observed induced magnetism, and the effect is clearly the most notorious for the (111) stacking, as discussed before. However, since quantum confinement also exists for the $n = 2$ cases, then why is their induced magnetism so weak even for the (111) stacking? Is this nearly vanishing moment a parametric "accident" for the (111) $n = 2$ SL, considering its spin-polarized DOS [Fig. 3(f)]? Our analysis suggests that this nontrivial behavior is caused by the particular quantum properties of this confined system. The (111)-stacking perovskite bilayer forms a honeycomb lattice that has a peculiar band structure.[36,37] In particular, for an isolated LNO bilayer there is a flat bottom band.[31–33] In the current study, although the LNO bilayer is not isolated in the crystal, its spin-down channel is effectively quantum confined. Then, the spin-down channel has a nearly flat bottom band (broadened since the barrier J_H is not infinitely high), which induces a large DOS peak at the band bottom [at -0.6 in Fig. 3(f)]. This occupied localized states can accumulate $0.5e_g$ spin-down electrons per Ni which significantly reduces the net induced magnetism. This tendency is clearly different from the $n = 1$ (111)-stacking case, where the large DOS peak [at 0.8 in Fig. 3(c)] due to the confinement is actually unoccupied.

It is also interesting to observe that this accident is fairly robust when modifying the parameters in reasonable ranges, as discussed in the following section. The underlying reason is that here the e_g electron density of Ni is higher than 1, while the nearly flat bottom band is always far below the Fermi level. In fact, in the vicinity of the Fermi level, there is no substantial difference between the spin-up and spin-down DOS. In summary, the weak induced magnetism for the $n = 2$ (111) stacking is also due to the quantum confinement.

All the results above were obtained for short periodic SLs, in which all Ni cations are interfacial. In thicker cases ($n \geqslant 3$), there are inner Ni layers that do not connect directly to Mn. Then their induced magnetism, if any, can be considered as a second-order effect of the quantum confinement. As shown in Fig. 4, the induced magnetism in these cases displays an interesting modulation as a function of the distance from the interfaces.[37] As expressed before, the induced magnetization in the (001)-stacking SLs is always weak, irrespective of the period n. Therefore, the (001)-stacking LNO/LMO should not present a robust exchange bias, in agreement with experiments.[24] By contrast, the (111)-stacking SLs display the largest induced magnetization, with the caveat that it nearly vanishes at $n = 2$ for the reasons already explained. When $n \geqslant 3$, the (111) magnetization of the first layer fluctuates around $0.1\mu_B \sim 0.2\mu_B$ per Ni, while the second Ni layers shows negative magnetization $\sim -0.1\mu_B$ per Ni. For deeper Ni-layers (3rd, 4th, 5th, and more) the magnetic moments become weaker and weaker, finally fluctuate around zero and approaching the PM state of pure LNO. This qualitatively explains the decreasing exchange bias with increasing period n when $n \geqslant 5$ (corresponding to the appearance of the third layers) observed in experiments.[24]

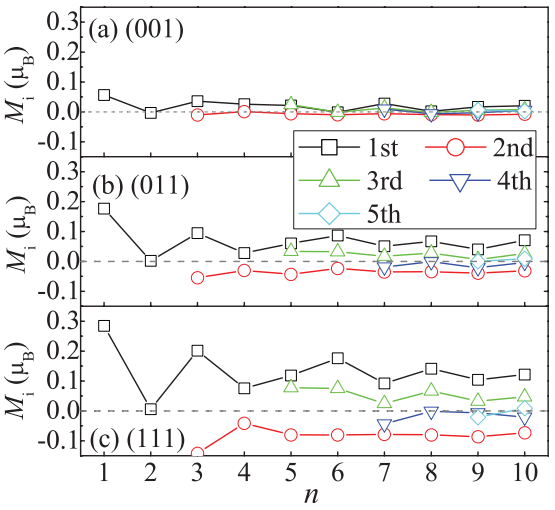

FIG. 4. (Color online) Magnetization profiles vs distances from the interfaces (e.g., the "1st" curves denote the first interfacial layers). A higher index denotes deeper LNO layers. $V_{Ni} = U = 0$ is used. The stackings are (001) in panel (a), (011) in panel (b), and (111) in panel (c).

Despite the previously described agreement of the interfacial induced magnetism between our model and the DFT studies,[24] these two techniques have a sign difference regarding the induced moments in middle layers of long periodic SLs ($n > 5$). This discrepancy needs further studies involving both experimental and theoretical components.

B. Correlated effect and other V_{Ni}

Our results above were obtained with $V_{Ni} = U = 0$. It is necessary to confirm the robustness of those results with other parameters since real SLs may correspond to another set of values for V_{Ni} and U. For example, previous DFT studies reported induced moments larger than those found in our study described above,[24] and this may be caused by the influence of correlation effects.

By varying V_{Ni} parametric with $U = 2$, the e_g density and e_g magnetization of short periodic SLs are shown in Fig. 5. Clearly, in all cases, the more negative V_{Ni} becomes, the more e_g electrons accumulate on the Ni layers. Regarding the induced magnetism, varying V_{Ni} the induced magnetization remains qualitatively robust. In the $n = 1$ cases, the induced moment of Ni is quite weak in the (001) stacking but prominent in the (111) stacking, as in the $U = 0$ case. With this Hubbard-type correlation effect, the induced moments in the (111) $n = 1$ case are significantly enhanced; a result comparable with the DFT data.

Another effect of the Hubbard interaction is the suppression of the charge leakage from Mn to Ni. For example, in the $n = 1$ case, when $U = 2$ and $V_{Ni} = 0$, the e_g density of Ni is close to the original value 1, implying a very weak charge transfer. However, the induced magnetization remains quite prominent, further confirming that the charge leakage from Mn to Ni is *not* the key origin of the induced magnetization in the Ni layers. In the $n = 2$ case, all induced magnetic moments are very weak, although not exactly zero, even with the Hubbard interaction.

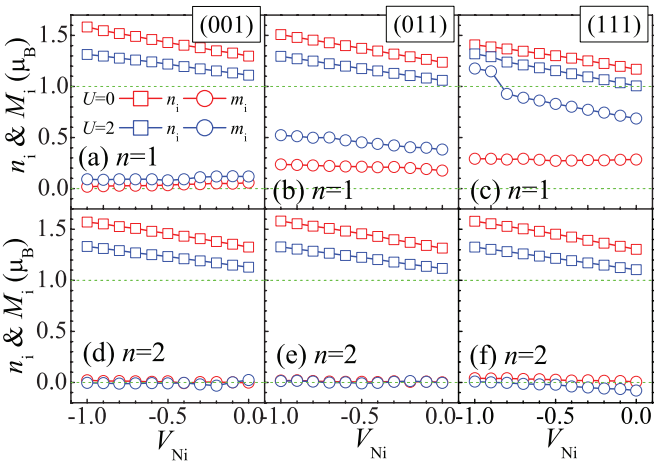

FIG. 5. (Color online) Ni e_g electron densities (squares) and magnetization (circles) versus V_{Ni} for $U = 0$ (red) and $U = 2$ (blue). Top row shows $n = 1$, bottom row shows $n = 2$. Left, middle, and right panels show (001), (011), and (111) stacking, respectively.

All these results imply that quantum confinement effects are qualitatively robust within a reasonable parameter region.

The results for thicker SLs ($n \geqslant 3$) show similar behavior, with positive induced magnetic moments for the first interfacial layers followed by weaker negative ones for the second layers. The thickness-dependent modulation, which is also similar to the noncorrelated limit, is also calculated in the case of thicker SLs with correlation couplings ($U = 2$ and $V_{Ni} = -1$), as shown in Fig. 6. Comparing with Fig. 4 in the noncorrelated limit, no qualitative differences are observed, although the values of the induced magnetic moments are enhanced due to the correlation effects. Thus, the oscillatory characteristics of the induced magnetism with an increasing distance from the interfaces is a robust feature of our results.

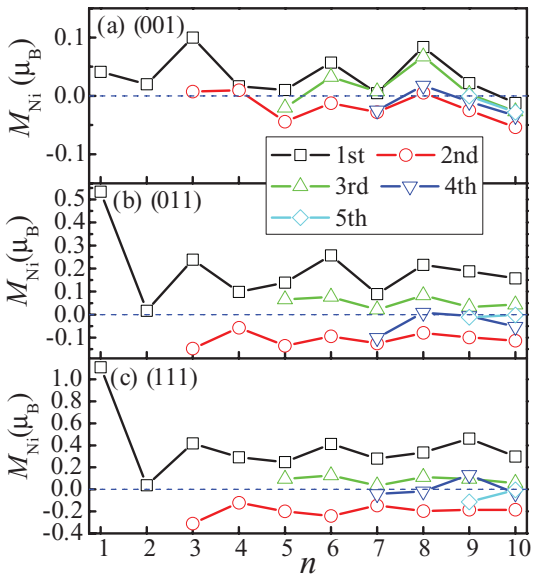

FIG. 6. (Color online) Magnetization profiles vs distance from interface. $V_{Ni} = -1$, $U = 2$ are used. All notations are the same as in Fig. 4.

C. Ruderman-Kittel-Kasuya-Yosida-like exchange

In Figs. 4 and 6, two features of the induced magnetization are worth highlighting: (1) the sign oscillations with increasing distance from the interfaces and (2) the fluctuations of the values of the first/second layers with increasing period n, both suggestive of a Ruderman-Kittel-Kasuya-Yosida-like (RKKY-like) exchange coupling between the LNO and LMO layers. In this sense, the almost vanishing magnetism of the LNO bilayer $n = 2$ can also be qualitatively understood: the first Ni layer of the left interface is also the second layer counting from the right interface, leading to a partial cancellation of the net magnetization. This RKKY-based description, which qualitatively agrees with the previously described explanation based on band structures, provides a more intuitive understanding than the rather complex calculations and results presented thus far.

To confirm this idea, the induced magnetization was recalculated by flipping the magnetic background of some Mn layers in the (111)-stacking $n = 2$ case. Two situations were tested: (1) flipping one layer in each bilayer (Mn↑-Mn↓-Ni-Ni-Mn↑-Mn↓); (2) flipping one bilayer entirely (Mn↓-Mn↓-Ni-Ni-Mn↑-Mn↑). Both these cases now give very prominent induced local magnetization in the LNO $n = 2$ bilayers, which couples antiferromagnetically between these two neighboring layers (-Ni↓-Ni↑-), as shown in Fig. 7. While this result is different from the ferromagnetically ordered case (Mn↑-Mn↑-Ni-Ni-Mn↑-Mn↑), it also supports the scenario of a RKKY coupling between the Mn's local moments and the Ni's induced moments.

If the magnetic coupling between LMO and LNO layers is indeed RKKY like, then an interesting question arises: How far can the coupling penetrate in these superlattices? To address this issue, the energy difference between FM and antiferromagnetic (AFM) $LaMnO_3$ layers was calculated varying the period n. Here, the AFM-coupled LMO layers denote the case Mn↓-· · · -Mn↓-Ni-· · · -Ni-Mn↑-· · · -Mn↑. As shown in Fig. 8, the absolute energy difference is large in short-period SLs, but it drops to nearly zero when $n \geqslant 5$. This tendency agrees with the results shown in Figs. 4(c) and 6(c),

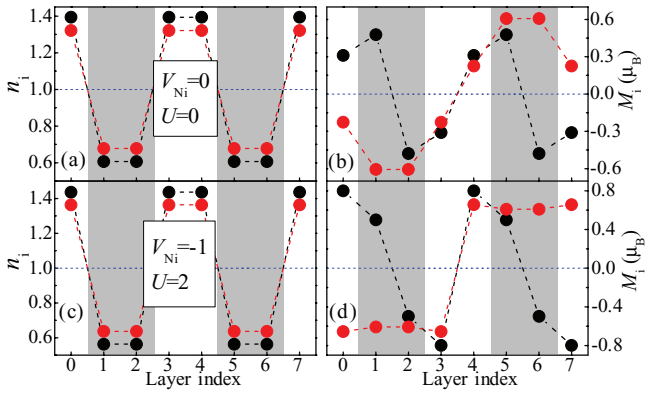

FIG. 7. (Color online) Profiles of e_g density (left) and e_g magnetization (right) for the $n = 2$ (111)-stacking superlattices with antiferromagnetically coupled $LaMnO_3$ layers. Black is for Mn↑-Mn↓-Ni-Ni-Mn↑-Mn↓ configuration, red is for Mn↓-Mn↓-Ni-Ni-Mn↑-Mn↑ configuration. Gray region is LMO, white region is LNO. Panels (a) and (b) are for $V_{Ni} = 0$ and $U = 0$, panels (c) and (d) are for $V_{Ni} = -1$ and $U = 2$.

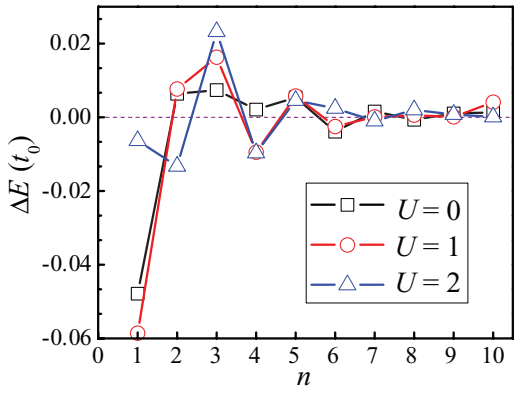

FIG. 8. (Color online) Energy differences per site between ferromagnetically coupled and antiferromagnetically coupled LMO layers ($E_{AFM} - E_{FM}$) in the (111)-stacking superlattices. $V_{Ni} = -1$ is used and U changes from 0 to 2.

where the induced magnetization becomes weak beyond the third layers (corresponding to the $n \geqslant 5$ cases). This result can qualitatively explain the experimentally observed decrease in the exchange bias with increasing period n for the case $n \geqslant 5$.[24]

D. Additional discussion

In the computational studies described above, the LMO layers were mainly set to have a fixed FM spin order, although a few simple AFM cases were also tested. This is reasonable considering the experimental evidence that clear FM hysteresis loops do appear in these SLs.[24] However, it is well known that there are various types of AFM phases in doped manganites, such as A-AFM, CE-AFM, G-AFM, and others, depending on the doping concentrations and bandwidths.[38–42] In the LMO-LNO SLs, if the charge leakage is very strong for some particular layers, it is possible to have any of these types of AFM orders, and considering all these possibilities is beyond the scope of the present effort.

It is interesting to compare the induced magnetism of the LMO/LNO SLs against the magnetic reconstruction observed in the LMO/SMO SLs that has been intensively investigated.[9–14] The induced magnetism in pure manganites SLs is associated with the magnetic phase transitions driven by the modification in the e_g density and strain.[12,14,43] Although not precisely in a one-to-one correspondence, in pure manganite SLs the induced magnetism can be traced back to the phase diagram of bulk manganites. By contrast, in the LMO/LNO SLs, although experiments also find a charge transfer from Mn to Ni,[24,44,45] the induced magnetization is nearly decoupled from this e_g electron transfer qualitatively different from the physics scenario in pure manganite SLs. Instead, here the physics for induced magnetization is more analogous to the dimensionality control of electronic phase transitions in LNO-$LaAlO_3$ heterostructures.[46,47]

It is also necessary to mention additional experimental observations. Despite the experiments of Gibert *et al.*, recent related experiments observed an exchange bias in the (001) stacking of $La_{0.75}Sr_{0.25}MnO_3$/LNO SLs,[44] as well as induced magnetism in (001)-stacked $(LMO)_2/(LNO)_n$ SLs,[45] which at least naively seem to disagree with the experiments of Gibert *et al.* and the present simulation. A probable reason for

this discrepancy may reside in the interfacial intermixing and disorder, which is unavoidable even in the best state-of-the-art experiments in the oxide-interfaces context. According to our quantum confinement mechanism, at least naively the disorder may enhance the induced magnetism since more Ni cations are at interfacial positions in situations of confinement. Of course, additional experimental and theoretical efforts are necessary in the future to clarify the role of disorder in this complex system. Certainly incorporating disorder effects is important but not an easy task in the computational studies due to the need to repeat the finite cluster calculations dozens of times for different disorder realizations and average the results to reach physically relevant results.

IV. CONCLUSION

The induced magnetization found in LNO in the LNO/LMO SLs was studied here via a hybrid microscopic model. The results of our model agree with previous DFT investigations[24] but provide additional details and a deeper physical insight. Summarizing our conclusions: (1) in the $n = 2$ SLs with FM LMO, the LNO layers are nearly nonmagnetic independent of the stacking directions. (2) The induced magnetization of LNO in the (111)-stacking SLs is always the most prominent. By contrast, the LNO layers in the (001)-stacking SLs are always nearly nonmagnetic, compatible with the exchange-bias investigations. The results for the (011) stacking are in between those of the (111) and (001) stackings, which can be verified in future experiments. (3) The induced magnetic moments of the first Ni layers are parallel to the moments of their nearest-neighbor Mn layers, but the second Ni layers usually display negative moments if not zero. The induced local magnetism decreases to zero in an oscillatory manner by increasing the thickness of the LNO layers. The underlying physical mechanism for the induced magnetization is associated with the spin-filtered quantum confinement supplemented by a RKKY-like exchange coupling, qualitatively different from the magnetization reconstruction in most previously studied oxide heterostructures. The present work reported here has emphasized more the approximately parameter-independent physical results, which may have a broader range of applications to related situations than the specific study of LMO/LNO may imply.

ACKNOWLEDGMENTS

We thank J.-M. Triscone, P. Zubko, M. Gibert, and A. Rüegg for helpful discussions. S. D. was supported by the 973 Projects of China (2011CB922101), NSFC (11004027, 11274060), NCET, and RFDP. The visit of S.D. to the University of Tennessee was supported in part by the National Science Foundation Grant No. DMR-1104386. E.D. was supported by the US DOE, Office of Basic Energy Sciences, Materials Sciences and Engineering Division.

[1] J. Mannhart and D. G. Schlom, Science **327**, 1607 (2010).
[2] H. Takagi and H. Y. Hwang, Science **327**, 1601 (2010).
[3] G. Hammerl and N. Spaldin, Science **332**, 922 (2011).
[4] E. Dagotto, Science **318**, 1076 (2007).
[5] M. Bibes, J. E. Villegas, and A. Barthélémy, Adv. Phys. **60**, 5 (2011).
[6] L. W. Martin, Y.-H. Chu, and R. Ramesh, Mater. Sci. Eng., R **68**, 89 (2010).
[7] P. Zubko, S. Gariglio, M. Gabay, P. Ghosez, and J.-M. Triscone, Annu. Rev. Condens. Matter Phys. **110**, 141 (2011).
[8] H. Y. Hwang, Y. Iwasa, M. Kawasaki, B. Keimer, N. Nagaosa, and Y. Tokura, Nat. Mater. **11**, 103 (2012).
[9] A. Bhattacharya, S. J. May, S. G. E. te Velthuis, M. Warusawithana, X. Zhai, B. Jiang, J.-M. Zuo, M. R. Fitzsimmons, S. D. Bader, and J. N. Eckstein, Phys. Rev. Lett. **100**, 257203 (2008).
[10] S. J. May, P. J. Ryan, J. L. Robertson, J.-W. Kim, T. S. Santos, E. Karapetrova, J. L. Zarestky, X. Zhai, S. G. E. te Velthuis, J. N. Eckstein, S. D. Bader, and A. Bhattacharya, Nat. Mater. **8**, 892 (2009).
[11] S. J. May, A. B. Shah, S. G. E. te Velthuis, M. R. Fitzsimmons, J. M. Zuo, X. Zhai, J. N. Eckstein, S. D. Bader, and A. Bhattacharya, Phys. Rev. B **77**, 174409 (2008).
[12] S. Dong, R. Yu, S. Yunoki, G. Alvarez, J.-M. Liu, and E. Dagotto, Phys. Rev. B **78**, 201102(R) (2008).
[13] Q. F. Zhang, S. Dong, B. L. Wang, and S. Yunoki, Phys. Rev. B **86**, 094403 (2012).
[14] S. Dong, Q. F. Zhang, S. Yunoki, J.-M. Liu, and E. Dagotto, Phys. Rev. B **86**, 205121 (2012).
[15] K. Ueda, H. Tabata, and T. Kawai, Science **280**, 1064 (1998).
[16] K. Ueda, H. Tabata, and T. Kawai, J. Appl. Phys. **89**, 2847 (2001).
[17] Y. Zhu, S. Dong, Q. Zhang, S. Yunoki, Y. Wang, and J.-M. Liu, J. Appl. Phys. **110**, 053916 (2011).
[18] P. Yu, J.-S. Lee, S. Okamoto, M. D. Rossell, M. Huijben, C.-H. Yang, Q. He, J. X. Zhang, S. Y. Yang, M. J. Lee, Q. M. Ramasse, R. Erni, Y.-H. Chu, D. A. Arena, C.-C. Kao, L. W. Martin, and R. Ramesh, Phys. Rev. Lett. **105**, 027201 (2010).
[19] C. A. F. Vaz, J. Hoffman, Y. Segal, J. W. Reiner, R. D. Grober, Z. Zhang, C. H. Ahn, and F. J. Walker, Phys. Rev. Lett. **104**, 127202 (2010).
[20] J. D. Burton and E. Y. Tsymbal, Phys. Rev. B **80**, 174406 (2009).
[21] J. D. Burton and E. Y. Tsymbal, Phys. Rev. Lett. **106**, 157203 (2011).
[22] M. J. Calderón, S. Liang, R. Yu, J. Salafranca, S. Dong, S. Yunoki, L. Brey, A. Moreo, and E. Dagotto, Phys. Rev. B **84**, 024422 (2011).
[23] S. Dong, X. T. Zhang, R. Yu, J.-M. Liu, and E. Dagotto, Phys. Rev. B **84**, 155117 (2011).
[24] M. Gibert, P. Zubko, R. Scherwitzl, J. Íñiguez, and J.-M. Triscone, Nat. Mater. **11**, 195 (2012).
[25] G. Catalan, Phase Transitions **81**, 729 (2008).
[26] E. Dagotto, T. Hotta, and A. Moreo, Phys. Rep. **344**, 1 (2001).
[27] E. Dagotto, New J. Phys. **7**, 67 (2005).
[28] T. Hotta and E. Dagotto, Phys. Rev. Lett. **92**, 227201 (2004).
[29] S. B. Lee, R. Chen, and L. Balents, Phys. Rev. B **84**, 165119 (2011).
[30] R. Yu, S. Yunoki, S. Dong, and E. Dagotto, Phys. Rev. B **80**, 125115 (2009).
[31] K.-Y. Yang, W. Zhu, D. Xiao, S. Okamoto, Z. Wang, and Y. Ran, Phys. Rev. B **84**, 201104(R) (2011).

[32] A. Rüegg and G. A. Fiete, Phys. Rev. B **84**, 201103(R) (2011).
[33] A. Rüegg, C. Mitra, A. A. Demkov, and G. A. Fiete, Phys. Rev. B **85**, 245131 (2012).
[34] C. Franchini, R. Kováčik, M. Marsman, S. S. Murthy, J. He, C. Ederer, and G. Kresse, J. Phys.: Condens. Matter **24**, 235602 (2012).
[35] E. Dagotto, *Nanoscale Phase Separation and Colossal Magnetoresistance* (Springer, Berlin, 2002).
[36] D. Xiao, W. Zhu, Y. Ran, N. Nagaosa, and S. Okamoto, Nat. Commun. **2**, 596 (2011).
[37] To simplify, the long-range Coulombic interaction due to charge transfer is neglected, which is acceptable if the period n is not too large and the dielectric constant is large.
[38] T. Hotta, S. Yunoki, M. Mayr, and E. Dagotto, Phys. Rev. B **60**, R15009 (1999).
[39] T. Hotta, M. Moraghebi, A. Feiguin, A. Moreo, S. Yunoki, and E. Dagotto, Phys. Rev. Lett. **90**, 247203 (2003).
[40] T. Hotta, Y. Takada, H. Koizumi, and E. Dagotto, Phys. Rev. Lett. **84**, 2477 (2000).
[41] S. Dong, R. Yu, S. Yunoki, J.-M. Liu, and E. Dagotto, Phys. Rev. B **78**, 064414 (2008).
[42] S. Dong, R. Yu, S. Yunoki, J.-M. Liu, and E. Dagotto, Phys. Rev. B **78**, 155121 (2008).
[43] R. Yu, S. Dong, C. Şen, G. Alvarez, and E. Dagotto, Phys. Rev. B **77**, 214434 (2008).
[44] J. C. Rojas Sánchez, B. Nelson-Cheeseman, M. Granada, E. Arenholz, and L. B. Steren, Phys. Rev. B **85**, 094427 (2012).
[45] J. Hoffman, I. C. Tung, B. Nelson-Cheeseman, M. Liu, J. Freeland, and A. Bhattacharya, arXiv:1301.7295.
[46] A. V. Boris, Y. Matiks, E. Benckiser, A. Frano, P. Popovich, V. Hinkov, P. Wochner, M. Castro-Colin, E. Detemple, V. K. Malik, C. Bernhard, T. Prokscha, A. Suter, Z. Salman, E. Morenzoni, G. Cristiani, H.-U. Habermeier, and B. Keimer, Science **332**, 937 (2011).
[47] J. Liu, S. Okamoto, M. van Veenendaal, M. Kareev, B. Gray, P. Ryan, J. W. Freeland, and J. Chakhalian, Phys. Rev. B **83**, 161102(R) (2011).